

RESEARCH

Open Access



Multistability and bifurcations in a 5D segmented disc dynamo with a curve of equilibria

Jianghong Bao^{1,2*} and Yongjian Liu²

*Correspondence:

majhbao@yahoo.com

¹School of Mathematics, South China University of Technology, Guangzhou, P.R. China

²Guangxi Colleges and Universities Key Laboratory of Complex System Optimization and Big Data Processing, Yulin Normal University, Yulin, P.R. China

Abstract

Multistability, i.e., coexisting attractors, is one of the most exciting phenomena in dynamical systems. This paper presents a new category of coexisting hidden attractor: five-dimensional (5D) systems with a curve of equilibria. Based on the segmented disc dynamo, a new 5D hyperchaotic system is proposed. The paper studies not only coexisting self-excited attractors but also coexisting hidden attractors in the new system with four types of equilibria: a curve of equilibria, a line equilibrium, a stable equilibrium, and no equilibria. Furthermore, the paper proves that the degenerate Hopf and pitchfork bifurcations occur in the system. Numerical simulations demonstrate the emergence of the two bifurcations.

Keywords: 5D segmented disc dynamo; Curve of equilibria; Multistability; Degenerate Hopf bifurcation; Pitchfork bifurcation

1 Introduction

Multistability or coexisting different attractors for a given set of parameters is one of the most exciting phenomena in dynamical systems [1]. Complex dynamical systems, ranging from human brain, climate, ecosystems to financial markets and engineering applications, typically have many coexisting attractors [2, 3]. High dimensional hyperchaotic systems describe natural phenomena more explicitly than low dimensional systems [4]. Nowadays the research of high dimensional multistability systems has captured attention of scientists from around the world.

Recently, it has been shown that multistability is connected with the occurrence of unpredictable attractors which have been called hidden attractors. Hidden attractors may cause disastrous events, such as sudden climate changes, serious diseases, financial crises, etc. [2, 5–7]. They are often related to dynamical systems with stable equilibria [8, 9], no equilibria [10, 11], a line equilibrium [12, 13], or a curve of equilibria [14–17]. A self-excited attractor has a basin of attraction associated with an unstable equilibrium. The classical attractors of Lorenz, Rössler, Chua, Chen, Sprott systems (cases B to S) are those excited from unstable equilibria [16]. This paper presents a new category of hidden attractor: five-dimensional (5D) systems with a curve of equilibria.

For the past few years, many dynamical systems have been reported to study curve-shaped equilibria [14–17]. Table 1 in Ref. [15] classifies the chaotic systems with an infinite

number of equilibria. However, it is noted that no 5D hyperchaotic systems with a curve of equilibria are reported in the literature.

Motivated by the above findings, the paper proposes a new 5D hyperchaotic system based on the segmented disc dynamo. We study not only coexisting self-excited attractors but also coexisting hidden attractors in the new system with four types of equilibria: a curve of equilibria, a line equilibrium, a stable equilibrium, and no equilibria. Further, we study the degenerate Hopf bifurcation and pitchfork bifurcation of the system by bifurcation theory [18, 19]. Numerical investigations are performed to verify the corresponding theoretical results for the two bifurcations.

The paper is organized as follows. Section 2 introduces a new 5D segmented disc dynamo with a curve of equilibria. Section 3 investigates different types of coexisting attractors. Section 4 investigates the degenerate Hopf bifurcation, and Sect. 5 analyzes the pitchfork bifurcation. Section 6 concludes the paper.

2 5D segmented disc dynamo with a curve of equilibria

2.1 Presentation of a 5D segmented disc dynamo with a curve of equilibria

Moffatt proposed the segmented disc dynamo which included the current associated with the radial diffusion of the magnetic field and satisfied the Alfvén theorem of flux conservation [20]:

$$\begin{cases} \dot{x}(t) = r(y - x), \\ \dot{y}(t) = mx - (1 + m)y + xz, \\ \dot{z}(t) = g(mx^2 + 1 - (1 + m)xy). \end{cases} \tag{2.1}$$

Based on (2.1), we translate z to $z - m$ and introduce new parameters, which result in the following 5D segmented disc dynamo:

$$\begin{cases} \dot{x}(t) = r(y - x), \\ \dot{y}(t) = xz - (1 + m)y + v, \\ \dot{z}(t) = g(mx^2 + 1 - (1 + m)xy) - k_1u + k_6z, \\ \dot{u}(t) = k_2y^2 - k_3z, \\ \dot{v}(t) = k_4x - xz + k_5v, \end{cases} \tag{2.2}$$

where r and m are positive parameters, and the others are real parameters.

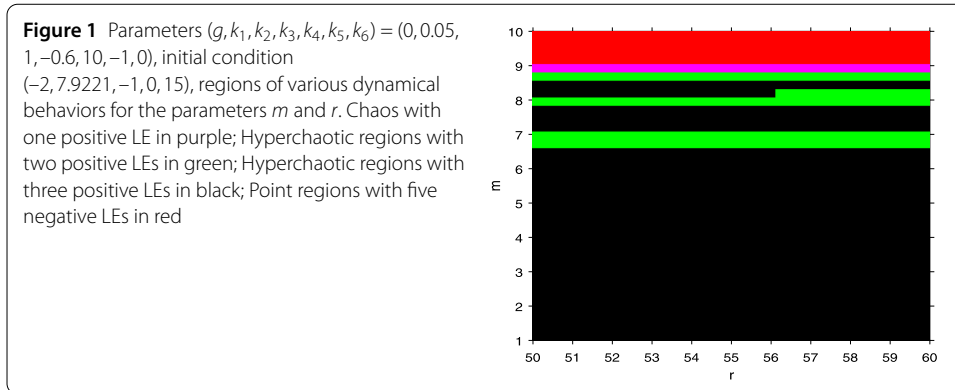
The divergence of the system is $\nabla \cdot V = -r - 1 - m + k_5 + k_6$, and the system is dissipative if $k_5 + k_6 < r + m + 1$. System (2.2) is invariant under the transformation $(x, y, z, u, v) \rightarrow (-x, -y, z, u, -v)$.

Now in order to obtain the hyperchaos with three positive Lyapunov exponents (LEs), we need to exclude some parameter sets that cannot make system (2.2) show bounded chaotic solutions.

Theorem 2.1 *If the following conditions are satisfied:*

$$g = k_2 = 0, \quad k_1 = k_3 - k_6 = r - k_4 = -1 - k_5 = m + 1 - r < 0, \tag{2.3}$$

then system (2.2) has no bounded chaotic or hyperchaotic solutions.



Proof From system (2.2), we can get

$$\dot{x} + \dot{y} + \dot{z} + \dot{u} + \dot{v} = (k_4 - r)x - (m + 1 - r)y - (k_3 - k_6)z - k_1u + (k_5 + 1)v. \tag{2.4}$$

By condition (2.3), Eq. (2.4) becomes

$$\dot{x} + \dot{y} + \dot{z} + \dot{u} + \dot{v} = (k_4 - r)(x + y + z + u + v).$$

Hence

$$x(t) + y(t) + z(t) + u(t) + v(t) = ce^{(k_4-r)t},$$

where c is an arbitrary constant. For $k_4 - r > 0$, system (2.1) is not chaotic because at least one of $x(t)$, $y(t)$, $z(t)$, $u(t)$, and $v(t)$ is not bounded.

Figure 1 shows the regions of various dynamical behaviors in the space of the parameters $(m, r) \in [1, 10] \times [50, 60]$ with the other fixed parameters $(g, k_1, k_2, k_3, k_4, k_5, k_6) = (0, 0.05, 1, -0.6, 10, -1, 0)$ and the initial condition $(-2, 7.9221, -1, 0, 15)$. Chaotic and hyperchaotic regions also include hidden chaos and hyperchaos. \square

2.2 Equilibria and stability

For $k_4 = 1 + m$, $k_5 = -1$, and $k_1k_3 \neq 0$, system (2.2) has a curve of equilibria

$$E_1 \left(x, x, \frac{k_2}{k_3}x^2, \frac{gk_3(1-x^2) + k_2k_6x^2}{k_1k_3}, (1+m)x - \frac{k_2}{k_3}x^3 \right).$$

We first discuss the case: $k_4 \neq 1 + m$ and $k_5 = -1$. For $k_1k_3 \neq 0$, there is an equilibrium $E_2(0, 0, 0, \frac{g}{k_1}, 0)$. For $k_1 = 0$ and $g \neq 0$, there is no equilibria. For $k_1 = g = 0$ or $k_3 = 0$, the system always has a line equilibrium. The other case, $k_4 = 1 + m$ and $k_5 \neq -1$, can be similarly discussed.

Let

$$S_1 = \left\{ (m, g, k_1, k_2, k_3, k_4, k_5, k_6) \left| \begin{array}{l} g = k_2 = 0, k_1k_3 \neq 0, k_4 = 1 + m, \\ k_5 = -1, k_6 < 0 \end{array} \right. \right\},$$

$$S_2 = \{(m, k_1, k_3, k_4, k_5, k_6) | k_1k_3 \neq 0, k_4 = 1 + m, k_5 < -1, k_6 < 0\},$$

and the following theorem is easily proved.

Theorem 2.2

- (1) *Suppose $(m, g, k_1, k_2, k_3, k_4, k_5, k_6) \in S_1$. If $k_1 k_3 > 0$, then the equilibrium E_1 of system (2.2) has at least three-dimensional stable manifold and one-dimensional unstable manifold. Otherwise, E_1 has at least four-dimensional stable manifold.*
- (2) *Suppose $(m, k_1, k_3, k_4, k_5, k_6) \in S_2$. If $k_1 k_3 > 0$, then the equilibrium E_2 is unstable and has four-dimensional stable manifold and one-dimensional unstable manifold. Otherwise, E_2 is stable and has five-dimensional stable manifold.*

3 Multistability

The complex dynamics of a hyperchaotic system are usually produced by the bifurcations at equilibria. However, curve-shaped equilibria are non-isolated and non-hyperbolic, so it is difficult to obtain the complex dynamics due to the bifurcation at equilibria. The methods of numerical analysis are vital for these systems with a curve of equilibria [14]. In addition, lots of other complex dynamics of system (2.2) are also discovered by means of the detailed numerical analysis.

3.1 Coexisting chaos and hyperchaos for system (2.2) with a curve of equilibria

When $(m, r, g, k_1, k_2, k_3, k_4, k_5, k_6) = (99, 9, 5, -10, 10, 10, 100, -1, 0)$, system (2.2) has a curve of equilibria $(x, x, x^2, \frac{1}{2}(x^2 - 1), 100x(1 - x^2))$. For the initial condition $(-2, 7.9221, -1, 0, 15.8407)$, system (2.2) has the LEs $(0.0095, 0.0017, 0, -10.5037, -22.3829)$, and the Kaplan–Yorke dimension is 3.0011. For the initial condition $(0.7513, 0.2551, 0.5060, 0.6991, 0.8909)$, the LEs are $(0.0038, 0, -0.0151, -10.1246, -17.2288)$, and the Kaplan–Yorke dimension is 2.2517. The hyperchaotic and chaotic attractors are shown in Fig. 2. Figure 2(c) shows the LEs spectrum with 200 varied initial conditions, and Fig. 2(d) shows the LEs spectrum for $r \in [7, 50]$ and the initial condition $(-2, 7.9221, -1, 0, 15.8407)$.

3.2 Coexisting chaos and hyperchaos for system (2.2) with no equilibria

When $(m, r, g, k_1, k_2, k_3, k_4, k_5, k_6) = (0.11, 8, 1.2, 0, 10, 0, -100, -1, 0)$, system (2.2) has no equilibria. For the initial condition $(-7.4047, -10.8076, 8.9184, -0.4523, 0.0641)$, the system has the LEs $(0.0062, 0, -0.0090, -0.0133, -10.0797)$, and the Kaplan–Yorke dimension is 2.6889. The chaos is shown in Fig. 3(a), and Fig. 3(b) shows the Poincaré map. For the initial condition $(-2, 0, 0.1, 0.1, 0)$, system (2.2) has the LEs $(0.0032, 0.0018, 0, -0.0123, -10.0995)$, and the Kaplan–Yorke dimension is 3.4065. A hyperchaotic attractor is shown in Fig. 3(c), and Fig. 3(d) shows the Poincaré map. Figure 3(e) shows the LEs spectrum with 200 varied initial conditions, and the corresponding Kaplan–Yorke dimensions are shown in Fig. 3(f).

3.3 Coexisting chaotic, quasiperiodic and periodic attractors for system (2.2) with a line equilibrium

When $(m, r, g, k_1, k_2, k_3, k_4, k_5, k_6) = (1.1, 6.1, 12, 0.1, 0, 0, -100, -1, 0)$, system (2.2) has a line equilibrium $(0, 0, z, 120, 0)$. For the initial condition $(100, -98, 100, 100, 100)$, the system has the LEs $(0.0058, 0, -0.0364, -2.3601, -6.8103)$. Figure 4(a) shows the chaotic attractor. For the initial condition $(-0.0506, -5.9116, 3.2069, -20.3950, 1.1477)$, the system has the LEs $(0, 0, -0.4492, -0.4526, -8.2991)$ and displays quasiperiodicity. For the initial condition $(2, 0.1, 0, 0, 0)$, a periodic attractor is shown in Fig. 4(b). Figure 4(c) shows the LEs spectrum with 200 varied initial conditions, and the corresponding Kaplan–Yorke dimensions are shown in Fig. 4(d).

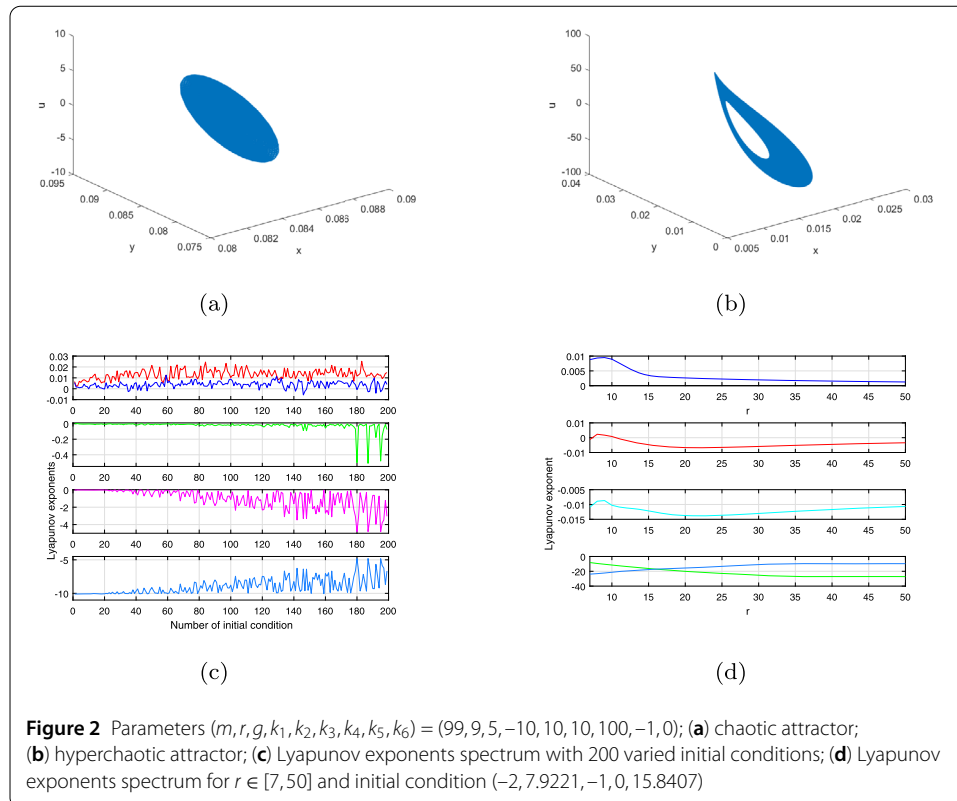


Figure 2 Parameters $(m, r, g, k_1, k_2, k_3, k_4, k_5, k_6) = (99, 9, 5, -10, 10, 10, 100, -1, 0)$; **(a)** chaotic attractor; **(b)** hyperchaotic attractor; **(c)** Lyapunov exponents spectrum with 200 varied initial conditions; **(d)** Lyapunov exponents spectrum for $r \in [7, 50]$ and initial condition $(-2, 7.9221, -1, 0, 15.8407)$

3.4 Coexisting chaos and hyperchaos for system (2.2) with a stable equilibrium

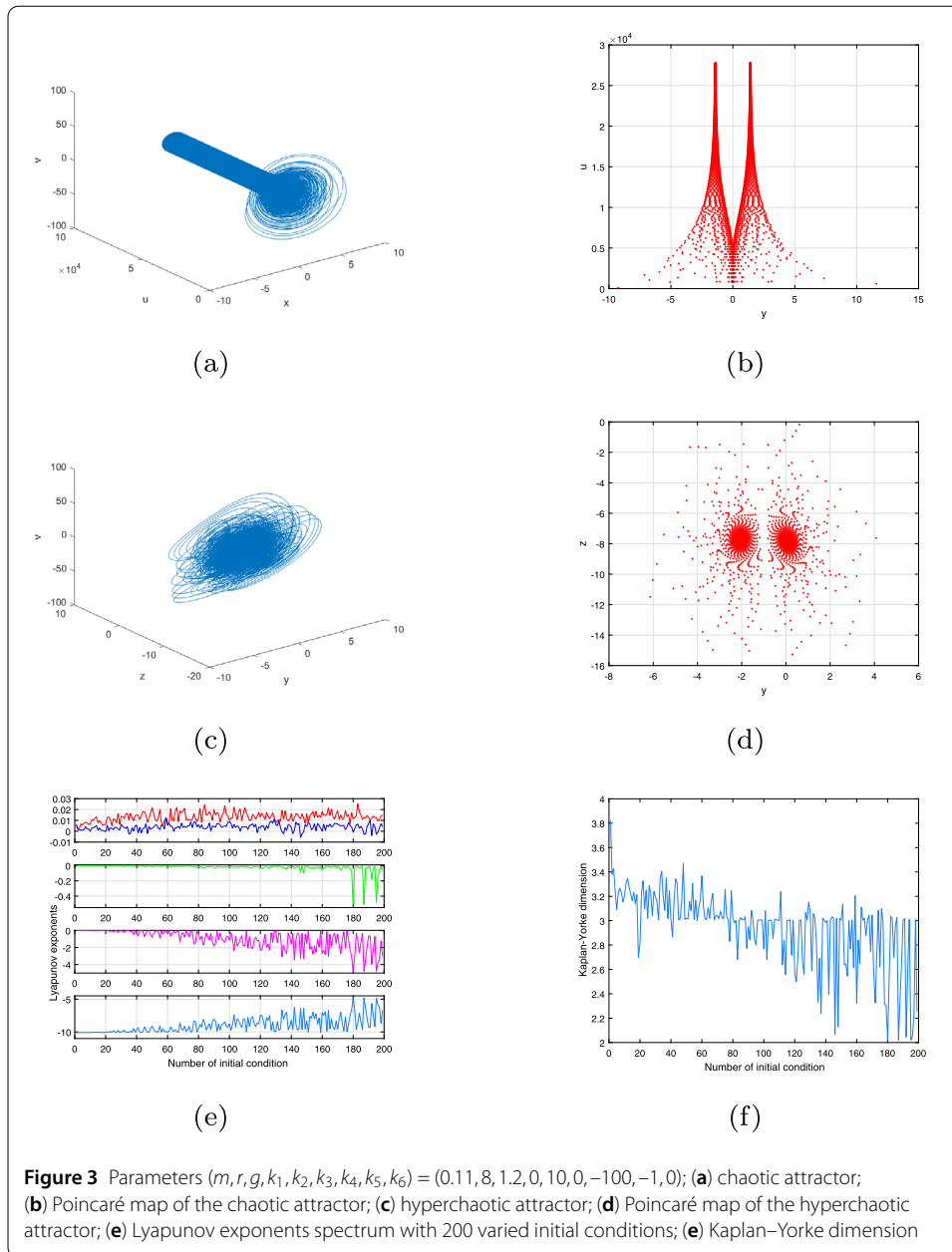
When $(m, r, g, k_1, k_2, k_3, k_4, k_5, k_6) = (1.3, 1, 0.12, 0.01, 0, -0.001, -1, 0, -0.001)$, system (2.2) has a stable equilibrium $(0, 0, 0, 12, 0)$. For the initial condition $(0.0326, 0.5612, 0.8819, 0.6692, 0.1904)$, the LEs are $(0.0031, 0, -0.0172, -0.0143, -3.2647)$. The chaotic attractor is shown in Fig. 5(a), and Fig. 5(b) shows the Poincaré map. For the initial condition $(0, 0, 0, 0, 0)$, the LEs are $(1.8956, 1.4008, 0, -0.0015, -6.5956)$, and the system displays hyperchaos.

3.5 Coexisting self-excited attractors

When $(m, r, g, k_1, k_2, k_3, k_4, k_5, k_6) = (1.3, 1, 12, 0.01, -0.1, -0.001, -2.3, -1, 0.1)$, system (2.2) has an unstable equilibrium $(0, 0, 0, 1200, 0)$. For the initial condition $(-0.3394, -64.0648, 91.0435, -75.5546, 10.5920)$, system (2.2) has the LEs $(0.0082, 0.0056, 0, -0.5393, -3.5561)$. A hyperchaotic attractor is obtained (see Fig. 6(a)), and the Poincaré map is shown in Fig. 6(b). For the initial condition $(0.1576, 0.9706, 0.9572, 0.4854, 0.8003)$, the system has the LEs $(0.0047, 0, -0.1228, -0.5298, -3.5469)$. The chaotic attractor is obtained in Fig. 6(c). The Poincaré map is shown in Fig. 6(d). When $r \in [1, 10]$, Fig. 7(a) shows the LEs spectrum, and the corresponding bifurcation diagram is shown in Fig. 7(b).

4 Degenerate Hopf bifurcation in system (2.2)

We utilize the projection method [18] to calculate the Lyapunov coefficients associated with Hopf bifurcation.



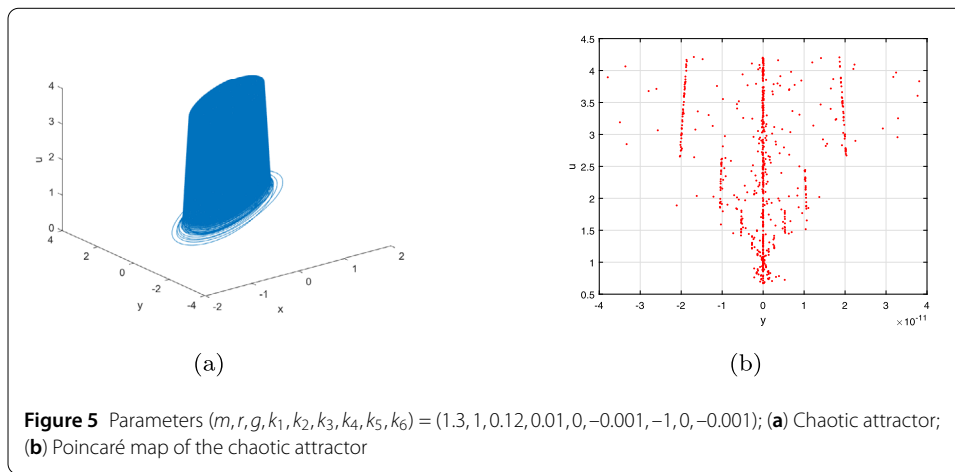
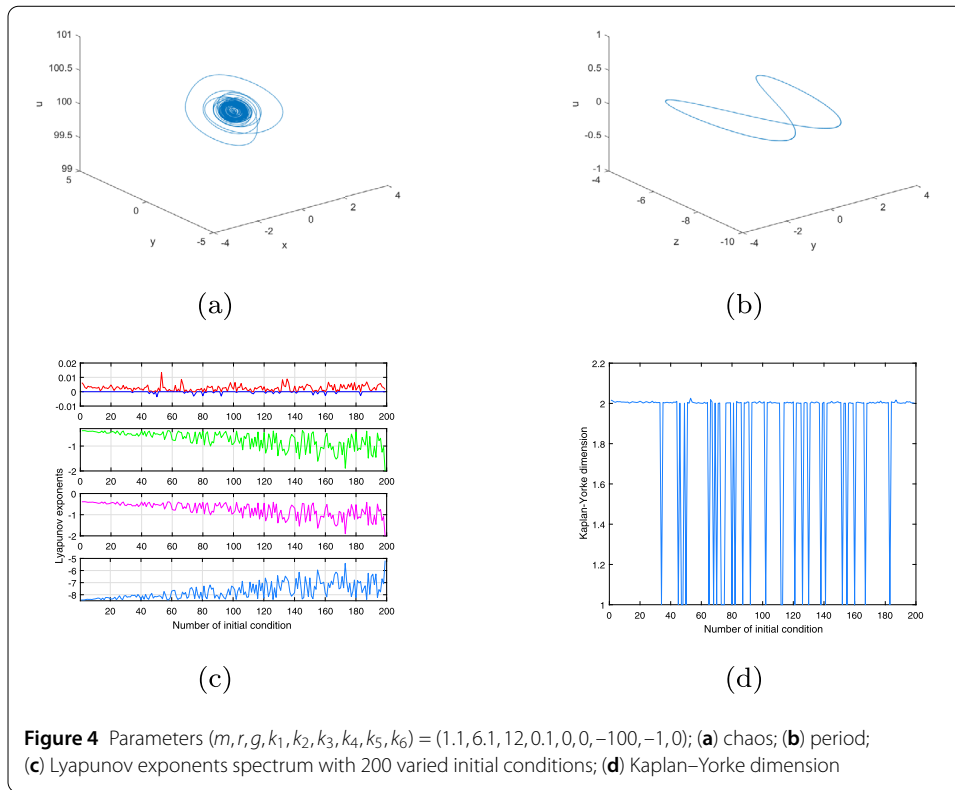
Let

$$\omega = \sqrt{-k_1 k_3},$$

$$S = \left\{ (m, r, g, k_1, k_2, k_3, k_4, k_5) \left| \begin{array}{l} m > 0, r > 0, k_2 = k_5 = 0, k_1 k_3 < 0, \\ g \neq 0, -(m + 1)(r + m + 1) < k_4 < 0 \end{array} \right. \right\}.$$

For $(m, r, g, k_1, k_2, k_3, k_4, k_5) \in S$, system (2.2) has only one equilibrium $E_2(0, 0, 0, \frac{g}{k_1}, 0)$. E_2 has the eigenvalues $\lambda(k_6) = \frac{k_6 \pm \sqrt{4k_1 k_3 + k_6^2}}{2}$, and the other eigenvalues of E_2 satisfy

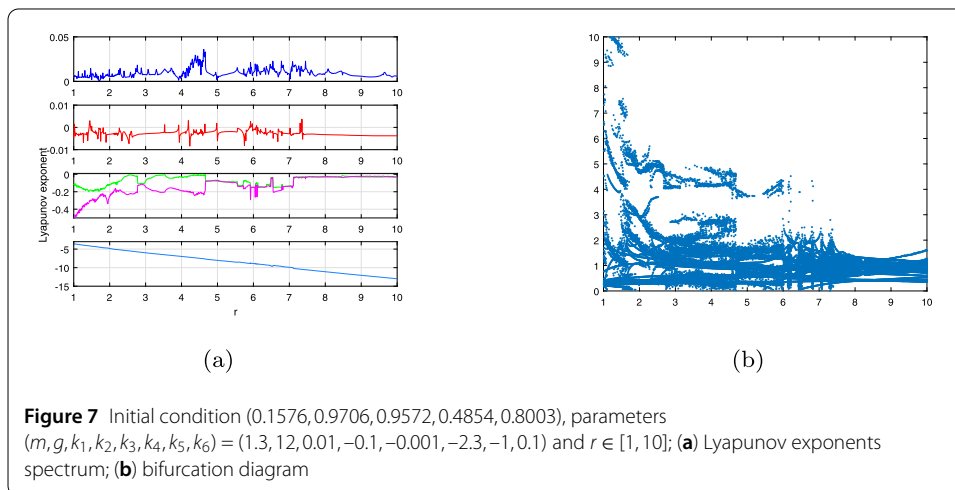
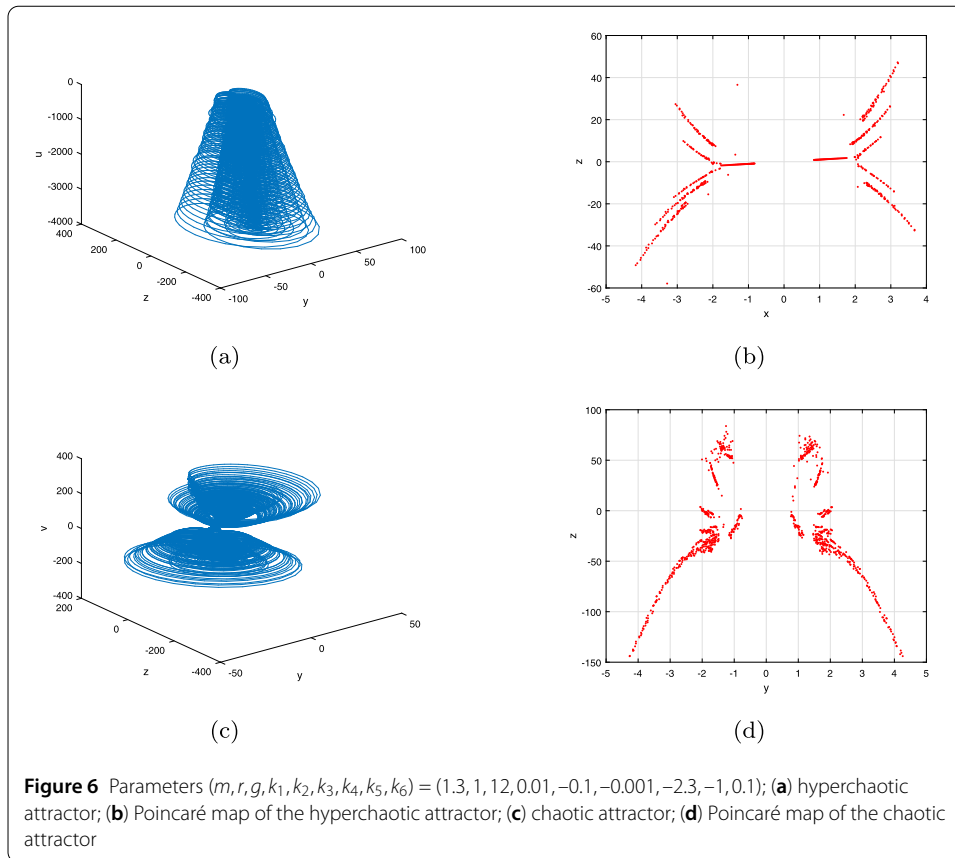
$$\lambda^3 + (1 + m + r)\lambda^2 + r(m + 1)\lambda - k_4 r = 0.$$



According to the Routh–Hurwitz criterion, the real parts of the roots λ are negative if and only if

$$\begin{aligned} \Delta_1 &= m + r + 1 > 0, \\ \Delta_2 &= r((m + 1)(r + m + 1) + k_4) > 0, \\ \Delta_3 &= -rk_4\Delta_2 > 0. \end{aligned}$$

When $k_6 = 0$ and $(m, r, g, k_1, k_2, k_3, k_4, k_5) \in S$, E_2 has a pair of purely imaginary eigenvalues $\pm\omega i$, and the other three eigenvalues with negative real part.



The transversality condition

$$\operatorname{Re}\left(\frac{d\lambda(k_6)}{dk_6}\right)\Big|_{k_6=0} = \frac{1}{2} > 0 \tag{4.1}$$

is also satisfied, and a Hopf bifurcation at E_2 occurs. We have the following theorem.

Theorem 4.1 *Considering system (2.2), for parameter $(m, r, g, k_1, k_2, k_3, k_4, k_5) \in S$ and $k_6 = 0$, the first and second Lyapunov coefficients $l_1 = l_2 = 0$ at E_2 , and the third Lyapunov coefficient is given by $l_3 = -\frac{4g((m+2)(m+1)+r(m-3))\omega^4+g(4r^2(m+2)+r(m+1)(k_4-m+3))\omega^2+gk_4r^2}{4(64\omega^6+16((m+1)^2+r^2)\omega^4+4((m+1)^2r^2+2k_4r(m+1+r))\omega^2+k_4^2r^2)}$.*

- (1) *If $l_3 > 0$, system (2.2) has a transversal Hopf point of codimension three at E_2 which is unstable.*
- (2) *If $l_3 < 0$, system (2.2) has a transversal Hopf point of codimension three at E_2 which is stable.*

Proof By the changes

$$\begin{cases} x = x, \\ y = y, \\ z = z, \\ u_1 = u - \frac{g}{k_1}, \\ v = v, \end{cases} \tag{4.2}$$

system (2.2) becomes the following system (still denoted by x, y, z, u, v):

$$\begin{cases} \dot{x}(t) = r(y - x), \\ \dot{y}(t) = xz - (1 + m)y + v, \\ \dot{z}(t) = g(mx^2 - (1 + m)xy) - k_1u + k_6z, \\ \dot{u}(t) = k_2y^2 - k_3z, \\ \dot{v}(t) = k_4x - xz + k_5v, \end{cases} \tag{4.3}$$

and the equilibrium $E_2(0, 0, 0, \frac{g}{k_1}, 0)$ is moved to $O(0, 0, 0, 0, 0)$.

From (4.1), the transversality condition holds. Now we calculate the Lyapunov coefficients, which show the stability of the equilibrium and the periodic orbit which appears.

According to Ref. [18], for the parameters $(m, r, g, k_1, k_2, k_3, k_4, k_5) \in S$ and $k_6 = 0$, we have

$$A = \begin{pmatrix} -r & r & 0 & 0 & 0 \\ 0 & -1 - m & 0 & 0 & 1 \\ 0 & 0 & 0 & -k_1 & 0 \\ 0 & 0 & -k_3 & 0 & 0 \\ k_4 & 0 & 0 & 0 & 0 \end{pmatrix},$$

$$p = \left(0, 0, -\frac{i}{2\omega}, \frac{1}{2k_3}, 0 \right),$$

$$q = (0, 0, -i\omega, k_3, 0),$$

$$B(X, Y) = (0, x_1y_3 + x_3y_1, 2gmx_1y_1 - g(1 + m)(x_1y_2 + x_2y_1), 0, -x_1y_3 - x_3y_1),$$

$$C = D = E = K = L = (0, 0, 0, 0, 0),$$

$$h_{11} = h_{20} = h_{22} = h_{30} = (0, 0, 0, 0, 0),$$

$$G_{21} = 0,$$

$$h_{21} = \left(1, \frac{i\omega + r}{r}, -\frac{i\omega}{k_3}, 1, \frac{(i\omega + 1 + m)(i\omega + r)}{r} \right),$$

$$\begin{aligned}
 h_{31} &= \left(\frac{3(2\omega + i)\omega r}{f(2)}, \frac{3i(2\omega - ir)(2\omega + i)\omega}{f(2)}, 0, 0, \right. \\
 &\quad \left. \frac{3i\omega(-4\omega^2 + 2i(m + r + 1)\omega + r(m + 1 - k_4))}{f(2)} \right), \\
 H_{32} &= \frac{6\omega^2 r b}{f(2)(2i\omega + 1 + m)(2i\omega + r)} (0, 1, 0, 0, -1), \\
 G_{32} &= 0,
 \end{aligned}$$

where

$$\begin{aligned}
 X &= (x_1, x_2, x_3, x_4, x_5), \quad Y = (y_1, y_2, y_3, y_4, y_5), \\
 f(n) &= -n^3\omega^3 i - n^2(m + r + 1)\omega^2 + nr(m + 1)\omega i - k_4 r.
 \end{aligned}$$

Therefore

$$l_1 = \frac{1}{2} \operatorname{Re}(G_{21}) = 0, \quad l_2 = \frac{1}{12} \operatorname{Re}(G_{32}) = 0.$$

Since $l_1 = l_2 = 0$, we continue to calculate l_3 . Some vector expressions are too complex, and for the convenience of expression, we write the results after calculation as follows:

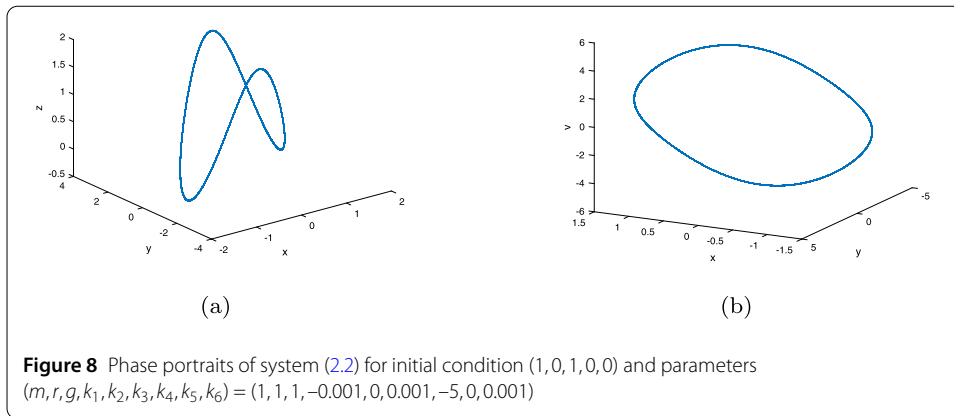
$$\begin{aligned}
 B(h_{11}, h_{32}) &= B(h_{20}, \bar{h}_{32}) = B(\bar{h}_{20}, h_{41}) = B(h_{21}, h_{22}) = B(h_{30}, \bar{h}_{31}) \\
 &= B(\bar{h}_{30}, h_{40}) = B(q, h_{33}) = (0, 0, 0, 0, 0), \\
 B(\bar{h}_{21}, h_{31}) &= \frac{-3b}{f(2)(2i\omega + 1 + m)(2i\omega + r)} \left(0, k_1 r, g\omega((m + 1)\omega - 2ri), 0, \frac{\omega^2 r}{k_3} \right), \\
 B(\bar{q}, h_{42}) &= \frac{4(2\omega + i)r\omega^2 i}{k_3 f(3)f(2)^2} (0, -c, 0, 0, c),
 \end{aligned}$$

where

$$\begin{aligned}
 b &= -8i\omega^3 - 4(m + r)\omega^2 + 2i(mr - m - 1)\omega - r(m + 1), \\
 c &= 216(k_3 + 3)\omega^6 - 180i(k_3 + 3)(1 + m + r)\omega^5 \\
 &\quad - 6((6(m + 1) + 25r)(m + 1)(k_3 + 3) + 18r^2)\omega^4 \\
 &\quad + 5ir((6(m + 2)(m + r) - 7k_4 + 6)(k_3 + 3) - 18r)\omega^3 \\
 &\quad + r((6mr(m + 2) - 13k_4(m + r + 1))(k_3 + 3) + 18r)\omega^2 \\
 &\quad + 5k_4(k_3 + 3)(1 + m)r^2\omega i - k_4^2 r^2(k_3 + 3).
 \end{aligned}$$

Hence one has $l_3 = -\frac{4g((m+2)(m+1)+r(m-3))\omega^4+g(4r^2(m+2)+r(m+1)(k_4-m+3))\omega^2+gk_4r^2}{4(64\omega^6+16((m+1)^2+r^2)\omega^4+4((m+1)^2r^2+2k_4r(m+1+r))\omega^2+k_4^2r^2)}$. □

Numerical simulation For $m = r = g = 1, k_2 = k_5 = 0, k_1 = -0.001, k_3 = 0.001, k_4 = -5$, and $k_6 = 0.001$, we have $l_3 = 0.05$. An unstable limit cycle is obtained with the initial condition $(1, 0, 1, 0, 0)$ (see Fig. 8).



5 Pitchfork bifurcation in system (2.2)

We utilize the center manifold theorem and the bifurcation theory [18, 19] to study pitchfork bifurcation of system (2.2).

Let

$$S = \{(k_1, k_2, k_3, k_4, k_5, k_6) | k_4 = k_5 = k_6 = 0, k_1 k_3 > 0, k_2 k_3 > 0\}.$$

When $(k_1, k_2, k_3, k_4, k_5, k_6) \in S$, system (2.2) has only one equilibrium $E_2(0, 0, 0, \frac{g}{k_1}, 0)$.

By the changes (4.2), system (2.2) becomes the following system (still denoted by x, y, z, u, v):

$$\begin{cases} \dot{x}(t) = r(y - x), \\ \dot{y}(t) = xz - (m + 1)y + v, \\ \dot{z}(t) = g(mx^2 - (1 + m)xy) - k_1u, \\ \dot{u}(t) = k_2y^2 - k_3z, \\ \dot{v}(t) = k_4x - xz, \end{cases} \tag{5.1}$$

and the equilibrium E_2 is moved to $O(0, 0, 0, 0, 0)$.

The Jacobian matrix at O is

$$J = \begin{pmatrix} -r & r & 0 & 0 & 0 \\ 0 & -m - 1 & 0 & 0 & 1 \\ 0 & 0 & 0 & -k_1 & 0 \\ 0 & 0 & -k_3 & 0 & 0 \\ 0 & 0 & 0 & 0 & 0 \end{pmatrix},$$

and the corresponding characteristic equation is

$$(\lambda^3 + (m + r + 1)\lambda^2 + (mr + r)\lambda)(\lambda^2 - k_1k_3) = 0.$$

System (2.2) has a zero eigenvalue $\lambda_1 = 0$ and the other four eigenvalues

$$\lambda_2 = -r, \quad \lambda_3 = -(m + 1), \quad \lambda_{4,5} = \pm\sqrt{k_1k_3}.$$

$O(0, 0, 0, 0, 0)$ is nonhyperbolic, and then we can get the following theorem.

Theorem 5.1 For $(k_1, k_2, k_3, k_4, k_5, k_6) \in S$, system (2.2) undergoes a pitchfork bifurcation at $E_2(0, 0, 0, \frac{r}{k_1}, 0)$. Furthermore, when $k_4 < 0$, there is only one equilibrium E_2 which is stable near the left-hand side of $k_4 = 0$; when $k_4 > 0$, E_2 becomes unstable and the other two equilibria are stable near the right-hand side of $k_4 = 0$.

Proof The corresponding eigenvectors are

$$\begin{aligned} \eta_1 &= \left(\frac{1}{m+1}, \frac{1}{m+1}, 0, 0, 1 \right)^T, \\ \eta_2 &= (1, 0, 0, 0, 0)^T, \\ \eta_3 &= \left(\frac{r}{r-m-1}, 1, 0, 0, 0 \right)^T, \\ \eta_4 &= \left(0, 0, -\frac{\sqrt{k_1 k_3}}{k_3}, 1, 0 \right)^T, \\ \eta_5 &= \left(0, 0, \frac{\sqrt{k_1 k_3}}{k_3}, 1, 0 \right)^T. \end{aligned}$$

Let

$$k_4 = \varepsilon, \quad T = (\eta_1, \eta_2, \eta_3, \eta_4, \eta_5), \quad (x, y, z, u, v)^T = T(x_1, y_1, z_1, u_1, v_1)^T. \tag{5.2}$$

By (5.2), system (5.1) becomes

$$\begin{cases} \begin{pmatrix} \dot{x}_1 \\ \dot{y}_1 \\ \dot{z}_1 \\ \dot{u}_1 \\ \dot{v}_1 \end{pmatrix} = \begin{pmatrix} 0 & 0 & 0 & 0 & 0 \\ 0 & -r & 0 & 0 & 0 \\ 0 & 0 & -(m+1) & 0 & 0 \\ 0 & 0 & 0 & \sqrt{k_1 k_3} & 0 \\ 0 & 0 & 0 & 0 & -\sqrt{k_1 k_3} \end{pmatrix} \begin{pmatrix} x_1 \\ y_1 \\ z_1 \\ u_1 \\ v_1 \end{pmatrix} + \begin{pmatrix} g_1 \\ g_2 \\ g_3 \\ g_4 \\ g_5 \end{pmatrix}, \\ \dot{\varepsilon} = 0, \end{cases} \tag{5.3}$$

where

$$\begin{aligned} a &= \frac{x_1}{1+m} - \frac{ry_1}{1+m-r} + z_1, \\ b &= \frac{k_1 v_1 a}{\sqrt{k_1 k_3}} (v_1 - u_1), \\ g_1 &= \varepsilon a - b, \\ g_2 &= \frac{b(m+2) - \varepsilon a}{m+1}, \\ g_3 &= \frac{(r+1)b - \varepsilon a}{m+1-r}, \\ g_4 &= \frac{1}{2} k_2 \left(\frac{x_1 + (1+m)y_1}{1+m} \right)^2 - \frac{ga\sqrt{k_1 k_3}(ma - (x_1 + (1+m)y_1))}{2k_1}, \\ g_5 &= \frac{1}{2} k_2 \left(\frac{x_1 + (1+m)y_1}{1+m} \right)^2 + \frac{ga\sqrt{k_1 k_3}(ma - (x_1 + (1+m)y_1))}{2k_1}. \end{aligned}$$

From the center manifold theorem, there exists a center manifold for Eqs. (5.3), which can be expressed locally as the following set through the variable x_1 and ε :

$$W_c(0) = \{(x_1, y_1, z_1, u_1, v_1, \varepsilon) | y_1 = h_1(x_1, \varepsilon), z_1 = h_2(x_1, \varepsilon), u_1 = h_3(x_1, \varepsilon), v_1 = h_4(x_1, \varepsilon), |x_1| < \delta, |\varepsilon| < \bar{\delta}, h_i(0, 0) = 0, Dh_i(0, 0) = 0, i = 1, 2, 3, 4\},$$

where δ and $\bar{\delta}$ are sufficiently small.

Assume that

$$\begin{cases} y_1 = h_1(x_1, \varepsilon) = a_1x_1^2 + a_2x_1\varepsilon + a_3\varepsilon^2 + o(3), \\ z_1 = h_2(x_1, \varepsilon) = b_1x_1^2 + b_2x_1\varepsilon + b_3\varepsilon^2 + o(3), \\ u_1 = h_3(x_1, \varepsilon) = c_1x_1^2 + c_2x_1\varepsilon + c_3\varepsilon^2 + o(3), \\ v_1 = h_4(x_1, \varepsilon) = d_1x_1^2 + d_2x_1\varepsilon + d_3\varepsilon^2 + o(3). \end{cases} \tag{5.4}$$

Considering $\dot{\varepsilon} \equiv 0$, the center manifold should satisfy

$$N(h(x_1, \varepsilon)) \triangleq D_{x_1}h \cdot g_1 - Bh - g \equiv 0, \tag{5.5}$$

where

$$h(x_1, \varepsilon) = \begin{pmatrix} h_1 \\ h_2 \\ h_3 \\ h_4 \end{pmatrix}, \quad D_{x_1}h = \begin{pmatrix} \frac{\partial h_1}{\partial x_1} \\ \frac{\partial h_2}{\partial x_1} \\ \frac{\partial h_3}{\partial x_1} \\ \frac{\partial h_4}{\partial x_1} \end{pmatrix}, \quad g = \begin{pmatrix} g_2 \\ g_3 \\ g_4 \\ g_5 \end{pmatrix},$$

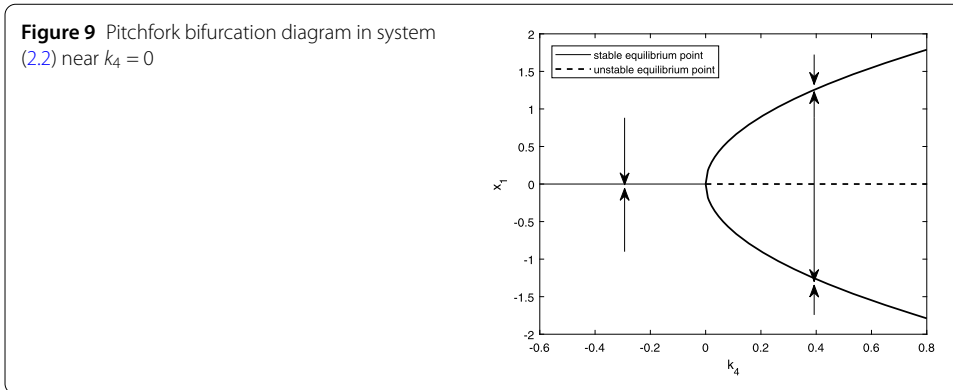
$$B = \begin{pmatrix} -r & 0 & 0 & 0 \\ 0 & -(m+1) & 0 & 0 \\ 0 & 0 & \sqrt{k_1k_3} & 0 \\ 0 & 0 & 0 & -\sqrt{k_1k_3} \end{pmatrix}.$$

Substituting Eqs. (5.4) to (5.5) gives

$$\begin{cases} a_1 = 0, & a_2 = -\frac{1}{(1+m)^3}, & a_3 = 0, \\ b_1 = 0, & b_2 = \frac{1}{(m+1)(r-m-1)r}, & b_3 = 0, \\ c_1 = -\frac{g\sqrt{k_1k_3}+k_1k_2}{2k_1\sqrt{k_1k_3}(1+m)^2}, & c_2 = 0, & c_3 = 0, \\ d_1 = \frac{k_1k_2-g\sqrt{k_1k_3}}{2k_1\sqrt{k_1k_3}(1+m)^2}, & d_2 = 0, & d_3 = 0, \end{cases}$$

and we obtain

$$\begin{cases} y_1 = h_1(x_1, \varepsilon) = -\frac{x_1\varepsilon}{(1+m)^3} + o(3), \\ z_1 = h_2(x_1, \varepsilon) = \frac{x_1\varepsilon}{(r-m-1)(m+1)r} + o(3), \\ u_1 = h_3(x_1, \varepsilon) = -\frac{(k_1k_2+g\sqrt{k_1k_3})x_1^2}{2k_1(1+m)^2\sqrt{k_1k_3}} + o(3), \\ v_1 = h_4(x_1, \varepsilon) = \frac{(k_1k_2-g\sqrt{k_1k_3})x_1^2}{2k_1(1+m)^2\sqrt{k_1k_3}} + o(3). \end{cases} \tag{5.6}$$



Applying Eqs. (5.6) into $\dot{x}_1 = g_1$ of (5.3) and reducing the vector field to the center manifold, we can get

$$\begin{cases} \dot{x}_1 = F(x_1, \varepsilon) + o(4), \\ \dot{\varepsilon} = 0, \end{cases} \tag{5.7}$$

where

$$F(x_1, \varepsilon) = \frac{(r(m + 1)^2 - (m + r + 1)\varepsilon)(k_3(m + 1)^2\varepsilon - k_2x_1^2)x_1}{k_3r(1 + m)^5}. \tag{5.8}$$

$F(x_1, \varepsilon)$ satisfies

$$\begin{cases} F(0, 0) = 0, & \frac{\partial F}{\partial x_1} |_{(0,0)} = 0, & \frac{\partial F}{\partial \varepsilon} |_{(0,0)} = 0, \\ \frac{\partial^2 F}{\partial x_1^2} |_{(0,0)} = 0, & \frac{\partial^2 F}{\partial x_1 \partial \varepsilon} |_{(0,0)} = \frac{1}{1+m} \neq 0, \\ \frac{\partial^3 F}{\partial x_1^3} |_{(0,0)} = -\frac{6k_2}{(1+m)^3 k_3} \neq 0, \end{cases}$$

which indicates that the equilibrium $(x_1, \varepsilon) = (0, 0)$ of Eqs. (5.7) undergoes a pitchfork bifurcation at $\varepsilon = 0$ ($k_4 = 0$). Since $-\frac{\partial^3 F}{\partial x_1^3} / \frac{\partial^2 F}{\partial x_1 \partial \varepsilon} > 0$, the bifurcation direction is near the right-hand side of $\varepsilon = 0$ ($k_4 = 0$). So Theorem 5.1 is proved. \square

Numerical simulation For $r = m = k_1 = k_2 = k_3 = 1$ and $g = k_5 = k_6 = 0$, (5.8) becomes

$$F(x_1, \varepsilon) = \frac{1}{32}(4 - 3\varepsilon)(4\varepsilon - x_1^2)x_1.$$

As shown in Fig. 9, system (2.2) undergoes a pitchfork bifurcation, which accords with Theorem 5.1.

6 Conclusions

The 5D segmented disc dynamo is very interesting and novel in that there are coexisting hidden attractors with four types of equilibria: a curve of equilibria, a line equilibrium, a stable equilibrium, and no equilibria. The paper studies not only coexisting self-excited attractors but also coexisting hidden attractors. Hidden hyperchaos with three positive

LEs is also displayed. Besides, by choosing an appropriate bifurcation parameter, the paper proves that the degenerate Hopf bifurcation and pitchfork bifurcation occur in the system. The simulation results demonstrate the correctness of the two bifurcations analysis.

The research on the new system may enrich the hyperchaotic theories and engineering applications. It is also hoped that the work is helpful to identify the geometrical characteristics of lower dimensional chaotic attractors. More studies will be explored to reveal the riddled property of the basin of attraction of the hyperchaotic attractors.

Acknowledgements

The authors would like to express many thanks to Professor Yuming Chen for his corrections and comments on this manuscript.

Funding

The research is supported by the Open Project of Guangxi Colleges and Universities Key Laboratory of Complex System Optimization and Big Data Processing (No. 2017CSOBPD0303) and the National Natural Science Foundation of China (No. 11671149).

Competing interests

The authors declare that they have no competing interests.

Authors' contributions

The authors have made the same contribution. All authors read and approved the final manuscript.

Publisher's Note

Springer Nature remains neutral with regard to jurisdictional claims in published maps and institutional affiliations.

Received: 20 November 2018 Accepted: 6 August 2019 Published online: 14 August 2019

References

1. Pisarchik, A.N., Feudel, U.: Control of multistability. *Phys. Rep.* **540**, 167–218 (2014)
2. Dudkowskia, D., Jafari, S., Kapitaniak, T., Kuznetsov, N.V., Leonov, G.A., Prasad, A.: Hidden attractors in dynamical systems. *Phys. Rep.* **637**, 1–50 (2016)
3. Liu, Y., Li, J., Wei, Z., Moroz, I.: Bifurcation analysis and integrability in the segmented disc dynamo with mechanical friction. *Adv. Differ. Equ.* **2018**, 210 (2018)
4. Ojoniyi, O.S., Njah, A.N.: A 5D hyperchaotic Sprott B system with coexisting hidden attractors. *Chaos Solitons Fractals* **87**, 172–181 (2016)
5. Abdel-Gawad, H.I., Saad, K.M.: On the behaviour of solutions of the two-cell cubic autocatalator reaction model. *ANZIAM J.* **44**, E1–E32 (2002)
6. Abdel-Gawad, H.I., Saad, K.M.: A chemotherapy-diffusion model for the cancer treatment and initial dose control. *Kyungpook Math. J.* **48**, 395–410 (2008)
7. Saad, K.M., Iyiola, O.S., Agarwal, P.: An effective homotopy analysis method to solve the cubic isothermal auto-catalytic chemical system. *AIMS Math.* **3**(1), 183–194 (2018)
8. Molaie, M., Jafari, S., Sprott, J.C., Golpayegani, S.M.R.H.: Simple chaotic flows with one stable equilibrium. *Int. J. Bifurc. Chaos Appl. Sci. Eng.* **23**, 1350188 (2013)
9. Wang, X., Chen, G.: A chaotic system with only one stable equilibrium. *Commun. Nonlinear Sci. Numer. Simul.* **17**, 1264–1272 (2012)
10. Pham, V.T., Volos, C., Jafari, S., Kapitaniak, T.: Coexistence of hidden chaotic attractors in a novel no-equilibrium system. *Nonlinear Dyn.* **87**, 2001–2010 (2017)
11. Jafari, S., Sprott, J.C., Golpayegani, S.M.R.H.: Elementary quadratic chaotic flows with no equilibria. *Phys. Lett. A* **377**, 699–702 (2013)
12. Jafari, S., Sprott, J.C.: Simple chaotic flows with a line equilibrium. *Chaos Solitons Fractals* **57**, 79–84 (2013)
13. Li, Q.D., Hu, S.Y., Tang, S., Zeng, G.: Hyperchaos and horseshoe in a 4D memristive system with a line of equilibria and its implementation. *Int. J. Circuit Theory Appl.* **42**, 1172–1188 (2014)
14. Chen, Y., Yang, Q.: A new Lorenz-type hyperchaotic system with a curve of equilibria. *Math. Comput. Simul.* **112**, 40–55 (2015)
15. Singh, J.P., Roy, B.K., Jafari, S.: New family of 4-D hyperchaotic and chaotic systems with quadric surfaces of equilibria. *Chaos Solitons Fractals* **106**, 243–257 (2018)
16. Barati, K., Jafari, S., Sprott, J.C., Pham, V.T.: Simple chaotic flows with a curve of equilibria. *Int. J. Bifurc. Chaos Appl. Sci. Eng.* **26**, 1630034 (2016)
17. Gotthans, T., Petržela, J.: New class of chaotic systems with circular equilibrium. *Nonlinear Dyn.* **81**, 1143–1149 (2015)
18. Kuznetsov, Y.A.: *Elements of Applied Bifurcation Theory*. Springer, New York (1998)
19. Wiggins, S.: *Introduction to Applied Nonlinear Dynamical Systems and Chaos*. Springer, New York (1990)
20. Moffatt, H.K.: A self-consistent treatment of simple dynamo systems. *Geophys. Astrophys. Fluid Dyn.* **14**, 147–166 (1979)